

NASA
CR
3080
c.1

NASA Contractor Report 3080

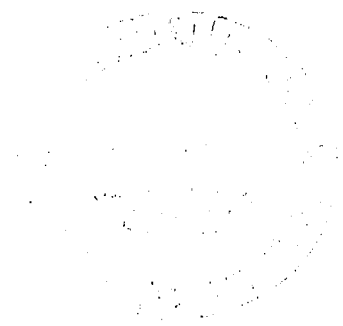
LOAN COPY: RETURN
AFWL TECHNICAL LIB
KIRTLAND AFB, NM

TECH LIBRARY KAFB, NM
0061884

Procedure for Noise Prediction and Optimization of Advanced Technology Propellers

Wen-Huei Jou and Samuel Bernstein

CONTRACT NAS2-9807
APRIL 1979





NASA Contractor Report 3080

Procedure for Noise Prediction and Optimization of Advanced Technology Propellers

Wen-Huei Jou and Samuel Bernstein
Flow Research Company
Kent, Washington

Prepared for
Ames Research Center
under Contract NAS2-9807

NASA

National Aeronautics
and Space Administration

**Scientific and Technical
Information Office**

1979

CONTENTS

	Page
TITLE PAGE	i
TABLE OF CONTENTS	ii
SUMMARY	1
INTRODUCTION	1
Propeller Noise Classification	2
THEORY OF BLADE PASSING TONE	3
PROPELLER NOISE WITH FORWARD FLIGHT	5
Retarded Potential Solution of Convected Wave Equation ...	5
Fourier Components of Acoustic Pressure	8
Zones of Relative Silence	15
Asymptotic Evaluation of Noise Field for Large Wave Number	18
OPTIMIZATION PROCEDURE FOR NOISE REDUCTION	21
General Noise Minimization Procedure	21
Approximate Noise Minimization Procedure	23
Noise Minimization for High-Frequency Noise	23
CONCLUSIONS	24
REFERENCES	25
THE APPENDIX	27

PROCEDURE FOR NOISE PREDICTION AND OPTIMIZATION OF

ADVANCED TECHNOLOGY PROPELLERS

Wen-Huei Jou and Samuel Bernstein
Flow Research Company

SUMMARY

The objectives of this work are to formulate a good method for predicting the noise field generated by an advanced technology propeller operating at supersonic tip speed and to formulate a noise minimization scheme for the design of the propeller blades. The work of Hawkins and Lowson on the noise prediction based on the Ffowcs Williams-Hawkins equation has been extended to include a forward flight velocity. The main idea for the extension is that the acoustic wave front propagates in a uniform flow as a convected and expanding sphere. Based on this, the fundamental solution of the convected wave equation can be easily obtained. Acoustic pressure at the observer's position is Fourier analyzed to give the frequency spectrum. The Fourier coefficients are expressed as integrals over the sources on the blade surface. The results show that cones of silence exist fore and aft the rotor plane with the semiapex angle $\Omega_s = \sin^{-1} \frac{1}{M_{tip}}$, where M_{tip} is the tip Mach number. This semiapex angle is the same for the forward and backward cones and is independent of the flight Mach number. This result is confirmed by the computation of the ray path associated with the emitted Mach waves. The strength of the signal is further modified by the Doppler amplification factor $\left\{ (1 - M^2 \sin^2 \Omega)^{\frac{1}{2}} - M \cos \Omega \right\}^{-1}$ and is stronger on the downstream side. These explicit directivity features are believed to give better physical insight into the problem of noise generation.

An optimization scheme for the blade design is formulated. The practical application of the scheme depends on the ease of the prediction of the load distribution from flow field computation.

INTRODUCTION

The motivation behind the present interest in advanced propeller aircraft is provided by a potential fuel saving on the order of 15 percent over a turbofan-powered aircraft (Ref. 1). Over the past several years, NASA has sponsored several theoretical and experimental studies to explore the feasibility of implementing a new propeller design for a

flight Mach number of 0.8 at 30,000 feet. Several configurations of 8-blade (and more recently 10-blade) propellers have been studied, and while the required efficiency of these propellers appears achievable, the potential noise level associated with these designs is extremely high. Estimates of the expected noise level by Hamilton Standard and by Boeing (Refs. 2, 3) are on the order of 135 to 150 dB for a tip Mach number of 1.2.

The objective of this present work is to formulate a noise computation and optimization procedure to enable the investigation of propeller design changes to minimize the radiated noise. The analysis was directed towards the noise associated with the transonic and supersonic flow over the propeller, and it will be interfaced with the flow field computations currently underway at NASA Ames Research Center.

This effort was supported by Professor W. D. Hayes of Princeton University who served as a consultant on this project. Professor Hayes was primarily responsible for the discussion on wave kinematics.

Propeller Noise Classification

The noise generated by a propeller with supersonic tip speed can be classified into three categories:

(1) Multiple pure tone (MPT): This noise appears with a discrete spectrum at the shaft rotating frequency and its multiples, and it is a unique feature of a propeller with supersonic tip speed (Ref. 1, 2, 3, 4). It has been identified as being caused by the merging of the rotating shock waves as they propagate away from the blades. Due to imperfection of the blade pitch angle and spacing, there will be a slight difference in the strength of the shocks as they emerge from the blades. When the shocks propagate into the far field, the stronger shocks catch up with the weaker ones and they merge into a shock of higher strength. Eventually, the shocks merge into a single shock rotating at the shaft frequency. MPT is an important component in the turbine fan noise. However, with only 8- or 10-blade configurations considered for the transonic propeller, this component of noise occurs in the very far field where the noise level is sufficiently weak and does not cause any concern. Also, it is a component of the noise which is hard to eliminate. We shall not pursue MPT in this report.

(2) Wide band noise: This is noise with a continuous spectrum, and it is attributable to turbulence traversing the propeller. For supersonic propellers, the wide band noise is much lower than the blade passing tone discussed in the following paragraph.

(3) Blade passing tone (BPT): This is a discrete tone at the blade passing frequency and its multiples. It is the rotating steady-pressure distribution sweeping past the observer periodically at the

blade passing frequency. With supersonic tip speed, a Mach wave system is generated around the blade. The passing of this rotating Mach wave system through the observer is the main cause of the pronounced noise encountered with supersonic propellers. In the remainder of this report, we shall focus the discussion on this component of the noise.

THEORY OF BLADE PASSING TONE

The work of Gutin on the noise generated by an open rotor (Ref. 4) is the only theoretical work published before the late 1960's. The main reason is that propellers were then operating at the subsonic tip speed range; Gutin's theory gives a very good description of the noise field in subsonic fields.

With the increasing interest in propellers operating at transonic and supersonic tip speeds, Gutin's theory has been proved to be inadequate. As the tip speed approaches and exceeds sonic speed, the characteristic wavelength of the noise is no longer much larger than the blade dimensions, as implied by Gutin's theory. The concept of representing a blade by a rotating concentrated force for calculation of the noise field breaks down. The noise field now depends on the detailed distribution of the source strength on the blade.

The general theory of sound generated by a surface in arbitrary motion has been investigated by Ffowcs Williams and Hawkings (Ref 5). They start from Lighthill's equation for aeroacoustics, with additional source terms resulting from the assumption that the solid surface is a surface of discontinuity within which the fluid is stationary. The general solution can be constructed in terms of the fundamental solution of the forced wave equation. The general solution is cast in an integral form over both the space and time domain involving a Dirac delta function in the integrand. Now, the important concept is that the space-time domain can be viewed as a general, four-dimensional space over which the Dirac delta function projects the integral to a three-dimensional subspace. This three-dimensional subspace can be chosen at will for convenience, thus resulting in various forms of representation of the solution. One of the most important forms is the projection to the physical space domain.

The procedure results in the traditional retarded potential solution. The integrand for integration in the space domain is then shown to be singular when the relative velocity of the surface to the observer is at sonic speed. One may also project the four-dimensional integral to a surface of sphere collapsing at sonic speed toward the observer. This form of solution avoids the above mentioned singularity, but creates a new singularity when the solid surface is moving toward the field point at sonic speed with its normal in the direction of radiation.

Two major works have been published applying the general theory of Ffowcs Williams and Hawkings to the supersonic rotor noise. Hawkings and Lowson (Ref. 6) base their analysis on the retarded potential solution.

They solve the problem in the frequency space and construct a time-wave form from its Fourier components. The singularity in the integrand is shown to be integrable. The Fourier coefficients are obtained explicitly by using a far field approximation. This leads to an integral over the blade surface which is evaluated numerically.

The authors then go on to apply Whitham's theory of weak shock propagation to calculate the nonlinear distortion of a time-wave form as it propagates into the far field. They show that the nonlinear effects substantially alter the wave form (hence the spectrum), but have weak effects on the overall sound pressure level. Finally, Hawkings and Lowson conclude that the linear theory can be used as a prediction tool for the gross features of the acoustic field. Since we shall attempt to generalize Hawkings and Lowson's theory to include the forward flight, we will expand on some features of their theory in the course of our analysis.

Farassat and Brown (Ref. 7), on the other hand, take up the approach using the collapsing sphere solution of Ffowcs Williams and Hawkings's general theory. To obtain the time-wave form, a collapsing sphere, centered at the observer, is generated from infinity for each time step. As the sphere collapses, the intersection of the sphere and the rotating blade surface is computed. The intersection line traces a surface, and the noise for that time step is evaluated by integration over that surface. No far field approximation is made; the procedure is purely numerical. The noise field can be mapped out by calculating noise at different observers' positions.

For the purpose of optimization, we are more interested in a scheme which contains the following features:

- (1) Fast computation of the noise field even if some approximation must be made.
- (2) Some explicit directivity distribution as a guidance for choosing observer's position for noise minimization.
- (3) Correct prediction of the sensitivity of the noise field to propeller design parameters.

With this in mind, we have elected to use Hawkings and Lowson's approach in outlining a noise minimization procedure.

In the following section, we extend the work by Hawkings and Lowson to include a forward flight. The resulting analysis will be applied to compute the noise level at the aircraft cabin, which is one of the major concerns for the advanced propeller aircraft.

PROPELLER NOISE WITH FORWARD FLIGHT

Retarded Potential Solution of Convected Wave Equation

The basic idea in the following analysis is that the wave front propagates in the uniform flow as a convected sphere (Ref. 8). Based on this, we are able to construct fairly easily the fundamental solution of the convected wave equation and cast the general solution in an integral form.

Consider an acoustic disturbance generated at A and propagating in a medium with speed of sound a and convecting Mach number M . The signal propagates away from A as a convected sphere, as shown in Figure 1.

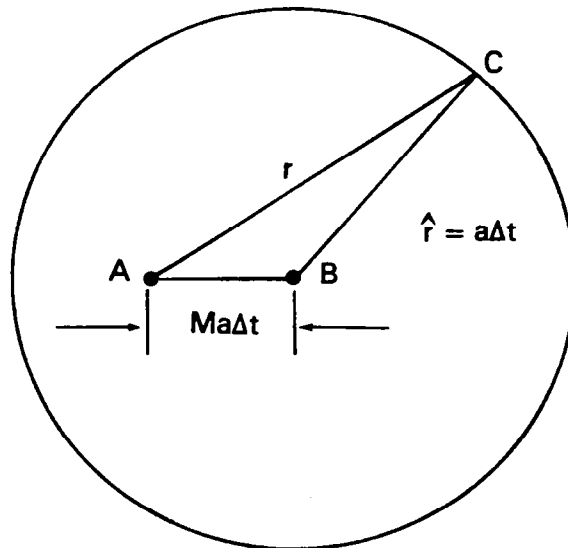


Figure 1. Wave Front Geometry.

The center of the convected spherical wave front is at B. For an observer at C, the received strength of the signal is proportional to \hat{r}^{-1} rather than r^{-1} . By simple geometry, the relation between r and \hat{r} can be obtained as

$$\frac{\hat{r}}{r} = (K^2 + \beta^2)^{\frac{1}{2}} - K, \quad (1)$$

where
$$K = (\vec{M} \cdot \vec{e}_r) \beta^2 \quad (2)$$

with
$$\beta = (1 - M^2)^{-1} \quad (3)$$

$$M^2 < 1. \quad (4)$$

The unit vector pointing from A toward C is \vec{e}_r . The retarded time to the observer at C is

$$\tau_o = t - \frac{\hat{r}}{a}. \quad (5)$$

The starting point of the subsequent analysis is that the solution to a convected Ffowcs Williams-Hawkings equation,

$$\frac{1}{a^2} \frac{D^2}{Dt^2} p - \nabla^2 p = \frac{\partial^n}{\partial x_i \partial x_j \dots} Q_{ij} \dots, \quad (6)$$

is the following:

$$4\pi(p - p_o) = \frac{\partial^n}{\partial x_i \partial x_j \dots} \int Q_{ij} \dots (\vec{y}, \tau) \frac{\Delta(\tau - \tau_o)}{\hat{r}} d\vec{y} d\tau, \quad (7)$$

with the relations (1) ~ (5).

In the preceding solution, the source space \vec{y} is described in a coordinate system fixed in space. The moving body (emitter) is viewed as distributed sources over the entire space and their strength is non-zero only when the solid body passes through that field point (\vec{y}). In other words, the sources are "pulsing sources" distributed in the entire source space.

In the case of the acoustic emission due to the thickness of and forces on the blade, the source space is chosen best in a coordinate fixed in the blade. The source strength described in such a coordinate system will be in a steady state. The acoustic signal at a point in the observer's space \vec{x} and at the observer's time t can then be obtained by summing the contributions of the steady sources emitted at the position related to the observer's space and time (\vec{x}, t) by the retarded time.

To do this, a transformation of the source space from the inertial frame \vec{y} to the blade fixed coordinate $\vec{\eta}$ is required. The transformation is given by:

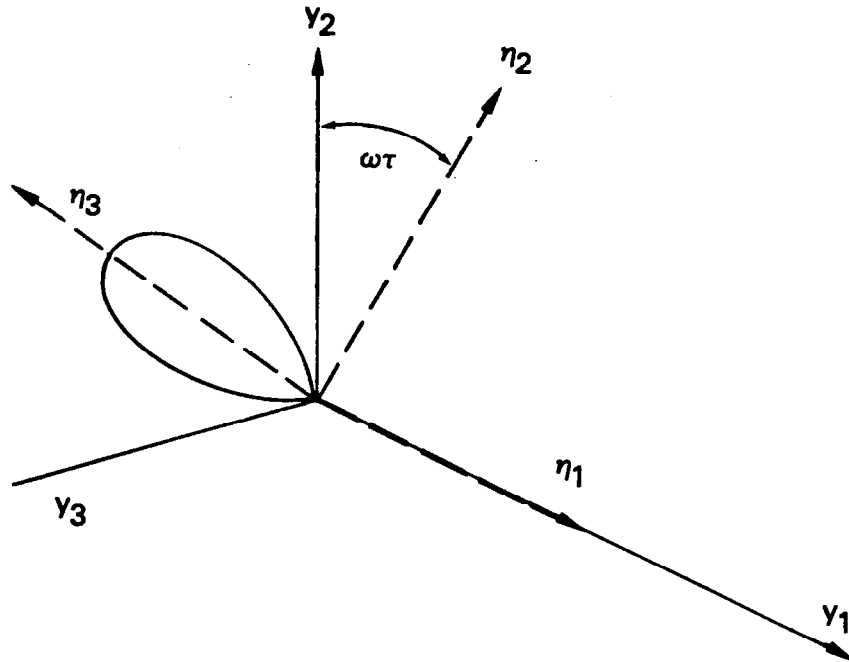


Figure 2. Blade Fixed Coordinate.

Where

$$y_1 = \eta_1 \quad ,$$

$$y_2 = \eta_3 \sin \omega \tau + \eta_2 \cos \omega \tau \quad ,$$

$$y_3 = \eta_3 \cos \omega \tau - \eta_2 \sin \omega \tau \quad ,$$

and

$$\tau = t - \frac{r}{a} \left\{ (K^2 + \beta^2)^{\frac{1}{2}} - K \right\} .$$

Without loss of generality, we assume the initial phase of the rotation is zero. Since r and \vec{e}_r depend on the variable \vec{y} , the above transformation is implicit. By some tedious calculations, it can be

shown that the Jacobian of the transformation is:

$$J = \det \left(\frac{\partial y_i}{\partial \eta_j} \right) = \frac{1}{(1 + U_i \frac{\partial \tau}{\partial y_i})} , \quad (8)$$

where U_i is the velocity of the emitter. Note that for $M=0$, so that $K=0$, and $\beta=1$, we recover the result shown by Ffowcs Williams and Hawkins (Ref. 5) and by Lawson (Ref. 9); i.e.,

$$J = \frac{1}{1 - \frac{\vec{U}}{a} \cdot \vec{e}_r} . \quad (9)$$

The acoustic pressure is then

$$4\pi(p - p_o) = - \frac{\partial}{\partial x_j} \int \left[\frac{f_j}{\hat{r}} J \right] dS - \frac{\partial}{\partial t} \int \left[\frac{\rho_o a (\vec{m} + \vec{M}) \cdot \nabla h}{\hat{r}} J \right] dS , \quad (10)$$

where $\left[\frac{f_j}{\hat{r}} J \right]$ denotes the values of the integrand at the retarded time, and the integration is evaluated over the blade surface. A thin blade is assumed, and we sum the force on the top and bottom surfaces of the blade. The net force on the planform of the blade is f_j ; the thickness of the blade is h ; and the rotation Mach number of the emitting element is \vec{m} .

Fourier Components of Acoustic Pressure

For the reasons mentioned in the Section "Theory of Blade Passing Tone" of this report, we follow Hawkins and Lawson's analysis (Ref. 6) and expand the solution in Fourier series. To convert the Fourier integral from being over the observer's time domain to the emitter's time domain, we have

$$\tau + \Delta t (\vec{y}(\tau)) = t , \quad (11)$$

so that

$$d\tau + \frac{dy_i}{d\tau} \frac{\partial(\Delta t)}{\partial y_i} d\tau = dt .$$

But,
$$\frac{dy_i}{d\tau} = U_i \quad \text{and} \quad \frac{\partial(\Delta t)}{\partial y_i} = \frac{\partial\tau}{\partial y_i} ,$$

so that
$$d\tau \left(1 + U_i \frac{\partial\tau}{\partial y_i} \right) = dt$$

or
$$dt = J^{-1} d\tau . \quad (12)$$

With this, the Fourier coefficients can be shown as

$$C_n = \frac{1}{4\pi} \int (in\omega I - \frac{\partial}{\partial x_j} I_j) dS , \quad (13)$$

where ω is the rotation frequency, n is the harmonic number, S is the blade surface,

$$I = \frac{\omega}{\pi} \int_0^{2\pi} \frac{\rho_0 a (\vec{m} + \vec{M}) \cdot \nabla h}{\hat{r}} \exp \left(in\omega \left(\tau + \frac{\hat{r}}{a} \right) \right) d\tau , \quad (14)$$

and
$$I_j = \frac{\omega}{\pi} \int_0^{2\pi} \frac{f_j}{r} \exp \left(in\omega \left(\tau + \frac{\hat{r}}{a} \right) \right) d\tau . \quad (15)$$

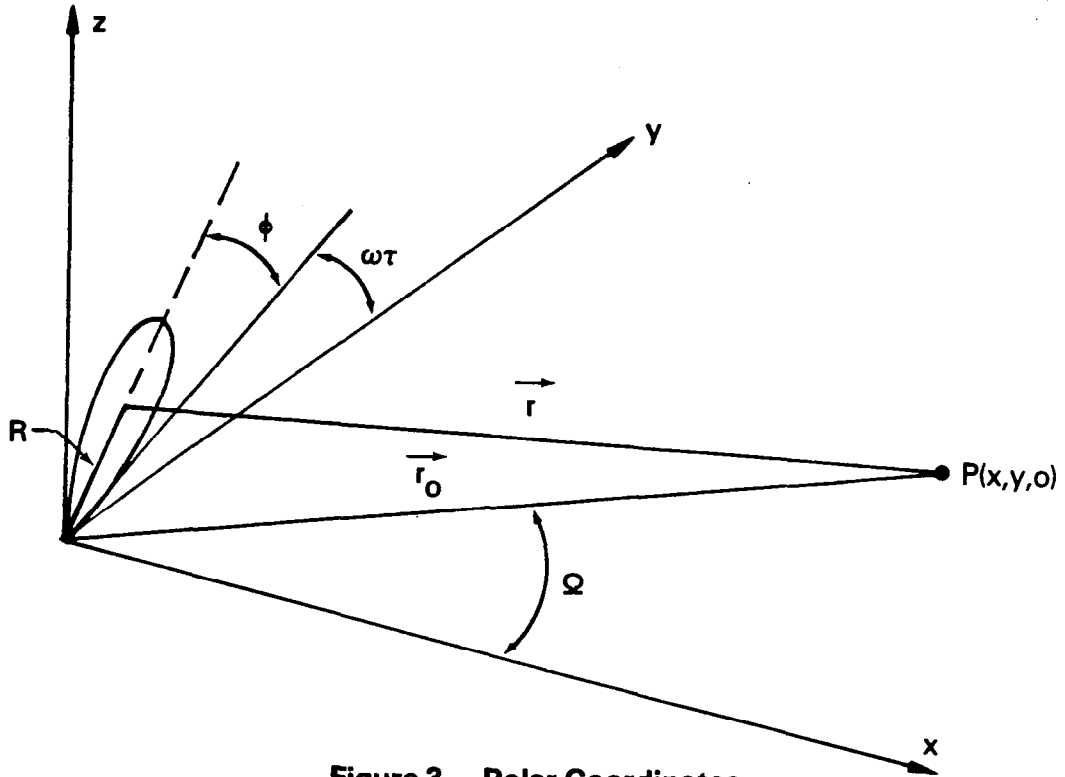


Figure 3. Polar Coordinates.

For a propeller with supersonic tip speed, the wave length $\frac{a}{n\omega}$ is comparable to the length of the blade R , since $\frac{\omega R}{a} \sim O(1)$. The source is noncompact, and it cannot be considered as a concentrated source even in the far field. However, we consider the far field approximation as the limit $R/r \ll 1$ and $\frac{a}{n\omega r} \ll 1$. The approximate expression for \hat{f} up to the first order is needed.

The acoustic field is axisymmetric and we shall consider an observer on x - y plane with position vector r_0 . Referring to Figure 3, we have

$$\hat{f} \approx \frac{r_0}{1 - M^2} \left\{ (1 - M^2 \sin^2 \Omega)^{\frac{1}{2}} - M \cos \Omega - \frac{(1 - M^2)}{(1 - M^2 \sin^2 \Omega)^{\frac{1}{2}}} \sin \Omega \cos \theta \frac{R}{r_0} \right\}. \quad (16)$$

So the exponential factor in equation (14) can be approximated by

$$E \equiv \exp \left(i\omega\tau + i\omega n \frac{\hat{r}}{a} \right)$$

$$\approx \exp \left\{ \frac{i n \omega}{a} \frac{r_0}{(1 - M^2)} \left[(1 - M^2 \sin^2 \Omega) - M \cos \Omega \right] \right\}$$

$$\cdot \exp \left\{ i\omega\tau - \frac{i n \omega R}{a} \frac{\sin \Omega \cos \theta}{(1 - M^2 \sin^2 \Omega)^{1/2}} \right\},$$

with $\theta = \omega\tau + \phi$

and $\sin \Omega = \frac{y}{r_0}$.

Let $\frac{\omega R}{a} = m$ be the rotation Mach number of the emitting element,

with $Y = \frac{m \sin \Omega}{(1 - M^2 \sin^2 \Omega)^{1/2}}$

and the Doppler factor

$$K_D = \left\{ (1 - M^2 \sin^2 \Omega)^{1/2} - M \cos \Omega \right\}.$$

We have*

$$I \approx \frac{2\rho_0 a (\vec{m} + \vec{M}) \cdot \nabla h (1 - M^2)}{r_0 K_D} \exp \left\{ \frac{i n \omega r_0}{a(1 - M^2)} K_D - i n \phi - \frac{i n \pi}{2} \right\} J_n(nY) \quad , \quad (17)$$

where J_n is the Bessel function. For the noise generated by the forces, we have

$$\begin{aligned} \frac{\partial I_j}{\partial x_j} &= \frac{\omega}{\pi} \int_0^{2\pi} f_j \frac{\partial}{\partial x_j} \left\{ \frac{1}{\hat{r}} \exp \left(i n \omega \left(\tau + \frac{\hat{r}}{a} \right) \right) \right\} d\tau \\ &= \frac{\omega}{\pi} \int_0^{2\pi} \exp \left(i n \omega \left(\tau + \frac{\hat{r}}{a} \right) \right) f_j \frac{\partial \hat{r}}{\partial x_j} \left(\frac{i \omega n}{a \hat{r}} - \frac{1}{\hat{r}^2} \right) d\tau \quad . \end{aligned}$$

For the far field $\frac{a}{n \omega \hat{r}} \ll 1$, we can neglect the last term in the last expression:

$$\frac{\partial I_j}{\partial x_j} = \frac{i n \omega^2}{a \pi} \int_0^{2\pi} \exp \left(i \omega n \left(\tau + \frac{\hat{r}}{a} \right) \right) \frac{f_j}{\hat{r}} \frac{\partial \hat{r}}{\partial x_j} d\tau \quad .$$

It can be shown that

$$\frac{1}{\hat{r}} \frac{\partial \hat{r}}{\partial x_j} \approx \frac{1}{K_D r_0} \left\{ \frac{\vec{e}_{r_0}}{(1 - M^2 \sin^2 \Omega)^{1/2}} - \frac{M^2 \sin \Omega}{(1 - M^2 \sin^2 \Omega)^{1/2}} \vec{j} - M \vec{i} \right\} .$$

The force on the blade is

$$f_j = (-T, -D \sin \theta, D \cos \theta) \quad ,$$

* $\frac{1}{\pi} \int_0^{\pi} \exp \xi i n - i n Y \sin \xi d\xi = J_n(nY)$

where T and D are respectively the thrust and drag components, so that

$$\vec{f} \cdot \vec{e}_r = -T \cos \Omega - D \sin \Omega \sin \theta ,$$

$$\frac{\vec{f} \cdot \nabla \hat{f}}{\hat{f}} = \frac{1}{K_D r_o (1 - M^2 \sin^2 \Omega)^{\frac{1}{2}}}$$

$$\left\{ T \left[-\cos \Omega + M(1 - M^2 \sin^2 \Omega)^{\frac{1}{2}} \right] - D \sin \Omega \sin \theta (1 - M^2) \right\} .$$

We have

$$\frac{\partial I_j}{\partial x_j} = \frac{i n \omega^2}{a \pi} \int_0^{2\pi} \omega \exp \left(i n \omega \left(\tau + \frac{\hat{f}}{a} \right) \right) \frac{1}{K_D r_o (1 - M^2 \sin^2 \Omega)^{\frac{1}{2}}}$$

$$\cdot \left\{ T \left[-\cos \Omega + M(1 - M^2 \sin^2 \Omega)^{\frac{1}{2}} \right] - D (1 - M^2) \sin \Omega \sin (\omega \tau + \phi) \right\} d\tau .$$

The thrust component is

$$\left(\frac{\partial I_j}{\partial x_j} \right)_T = \frac{2 i n \omega}{a} \frac{[-\cos \Omega + M(1 - M^2 \sin^2 \Omega)^{\frac{1}{2}}]}{K_D r_o (1 - M^2 \sin^2 \Omega)^{\frac{1}{2}}} T$$

$$\cdot \exp \left\{ \frac{i n \omega r_o}{a(1 - M^2)} K_D - i n \phi - \frac{i n \pi}{2} \right\} J_n(nY)$$

$$= -\frac{2 i n \omega}{a r_o K_D} \exp \left\{ \frac{i n \omega r_o}{a(1 - M^2)} - i n \phi - \frac{i n \pi}{2} \right\} J_n(nY)$$

$$\left\{ \frac{\cos \Omega}{(1 - M^2 \sin^2 \Omega)^{\frac{1}{2}}} - M \right\} T . \quad (18)$$

For the drag component we have

$$\left(\frac{\partial I_j}{\partial x_j} \right)_D = \frac{2in\omega}{a\pi} \frac{D(1-M^2) \sin \Omega}{K_D r_o (1-M^2 \sin^2 \Omega)^{1/2}} \exp \left\{ \frac{in\omega K_D r_o}{a(1-M^2)} - in\phi - \frac{in\pi}{2} \right\} \int_0^\pi \cos(n\xi - nY \sin \xi) \cos \xi d\xi .$$

But

$$\int_0^\pi \cos \xi \cos(n\xi - nY \sin \xi) d\xi$$

$$= \frac{1}{2} \int_0^\pi \left\{ \cos[(n+1)\xi - nY \sin \xi] + \cos[(n-1)\xi - nY \sin \xi] \right\} d\xi$$

$$= \frac{\pi}{2} \left\{ J_{n+1}(nY) + J_{n-1}(nY) \right\}$$

$$= \frac{\pi}{Y} J_n(nY) .$$

So,

$$\left(\frac{\partial I_j}{\partial x_j} \right)_D = \frac{2in\omega}{aK_D r_o} \frac{D(1-M^2)}{m} \exp \left\{ \frac{in\omega K_D r_o}{a(1-M^2)} - in\phi - \frac{in\pi}{2} \right\} \cdot J_n(nY) . \quad (19)$$

Substituting equations (17), (18) and (19) into equation (13), we have

$$C_n = \frac{in\omega}{2\pi a K_D r_o} \exp \left\{ \frac{in\omega r_o K_D}{a(1-M^2)} - \frac{in\pi}{2} \right\} \iiint \left\{ \rho_o a^2 (\vec{m} + \vec{M}) \cdot \nabla h (1-M^2) + T \left[\frac{\cos \Omega}{(1-M^2 \sin^2 \Omega)^{1/2}} - M \right] - \frac{D(1-M^2)}{m} \right\} J_n(nY) \exp(-in\phi) (\cos \Theta)^{-1} R dR d\phi \quad (20)$$

where m , T , D and h are functions of the coordinates (ϕ, R) on the blade surface, and θ is the twist angle.

We have reduced the Fourier coefficient of the noise at a point \vec{x} to a double integral on the blade planform surface.

One interesting feature of equation (20) can be observed. For fixed R , the ϕ integral is the Fourier integral of the thickness h and the forces T and D . With proper arrangement of the planform sweep, the R integration may give a favorable phase cancellation effect for those particular harmonics.

Zones of Relative Silence

Some of the directivity of the acoustic disturbance can be extracted from equation (20). In particular, the Bessel function $J_n(nY)$ is exponentially small for $Y < 1$. This is especially so for large n . So, $Y \leq 1$ defines a zone of relative silence (see Figure 4) in which only the subsonic Gutin noise exists:

$$Y^2 = \frac{m^2 \sin^2 \Omega}{1 - M^2 \sin^2 \Omega} \leq 1,$$

or
$$\Omega \leq \sin^{-1} \frac{1}{(m^2 + M^2)^{1/2}} = \sin^{-1} \frac{1}{M_{tip}}. \quad (21)$$

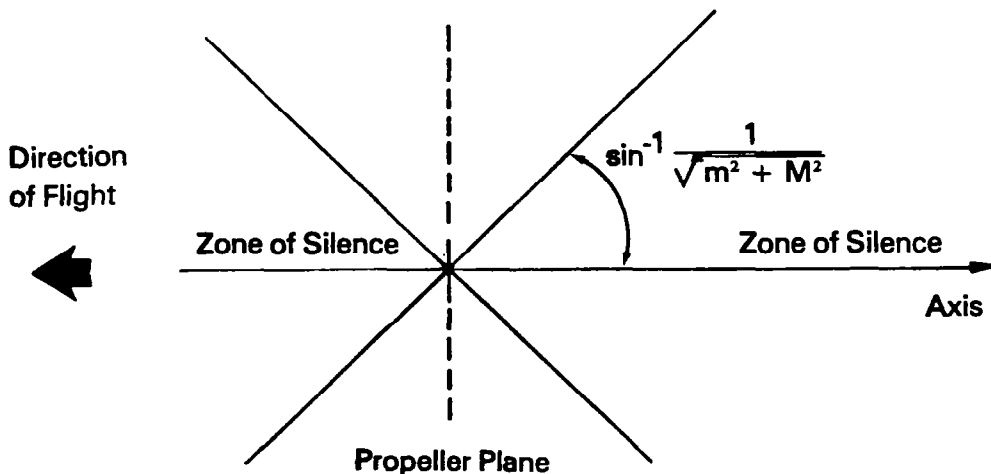


Figure 4. Zone of Silence.

This result is in agreement with the following kinematic consideration.

At each point on the supersonic portion of the blade, one can find the ray path of the acoustic waves.

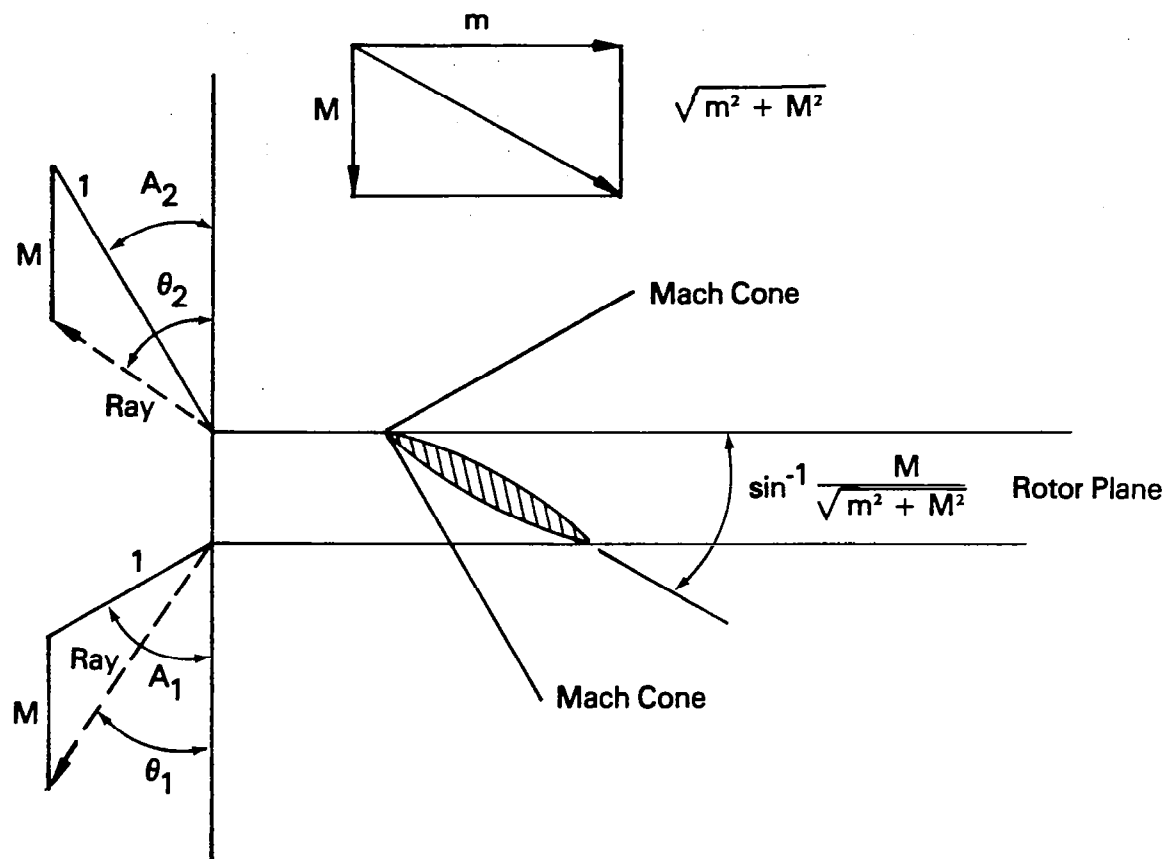


Figure 5. Ray Path.

Referring to Figure 5, we have

$$\angle A_1 = \sin^{-1} \frac{1}{(m^2 + M^2)^{1/2}} + \sin^{-1} \frac{M}{(m^2 + M^2)^{1/2}} \quad (22)$$

and

$$\angle A_2 = \sin^{-1} \frac{1}{(m^2 + M^2)^{1/2}} - \sin^{-1} \frac{M}{(m^2 + M^2)^{1/2}} \quad (23)$$

The ray angles downstream θ_1 and upstream θ_2 are given by the equation

$$\begin{aligned}
\tan \theta_{1,2} &= \frac{\sin \left\{ \sin^{-1} \frac{1}{(m^2 + M^2)^{\frac{1}{2}}} \pm \sin^{-1} \frac{M}{(m^2 + M^2)^{\frac{1}{2}}} \right\}}{\cos \left\{ \sin^{-1} \frac{1}{(m^2 + M^2)^{\frac{1}{2}}} \pm \sin^{-1} \frac{M}{(m^2 + M^2)^{\frac{1}{2}}} \right\}} \pm M \\
&= \frac{\frac{1}{(m^2 + M^2)^{\frac{1}{2}}} \left\{ \left(\frac{m^2}{m^2 + M^2} \right)^{\frac{1}{2}} \pm M \left(1 - \frac{1}{m^2 + M^2} \right)^{\frac{1}{2}} \right\}}{\left(\frac{m^2}{m^2 + M^2} \right)^{\frac{1}{2}} \left(1 - \frac{1}{m^2 + M^2} \right)^{\frac{1}{2}} \pm \frac{M}{m^2 + M^2} \pm M} \\
&= \frac{\frac{1}{m^2 + M^2}^{\frac{1}{2}}}{\left(1 - \frac{1}{m^2 + M^2} \right)^{\frac{1}{2}}} \cdot
\end{aligned} \tag{24}$$

We obtain thereby

$$\theta_1 = \theta_2 = \sin^{-1} \frac{1}{(m^2 + M^2)^{\frac{1}{2}}} \tag{25}$$

From equation (20), it can also be seen that the strength of the signal decays as $(K_D r_0)^{-1}$, where K_D is the Doppler factor which is dependent on the direction Ω as

$$K_D = (1 - M^2 \sin^2 \Omega)^{\frac{1}{2}} - M \cos \Omega \tag{26}$$

So, the strength of the signal is stronger on the downstream side as one would expect intuitively.

Figure 6 shows the qualitative directivity distribution from the forgoing discussion. A similar picture is obtained using kinematic consideration by Lowson and Jupe (Ref. 10).

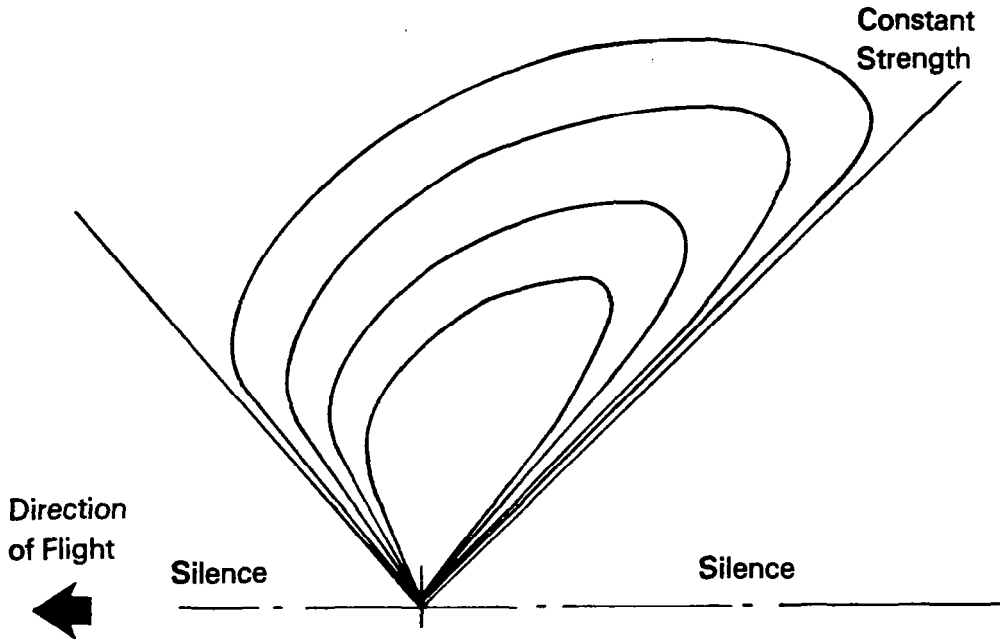


Figure 6. Qualitative Directivity.

Asymptotic Evaluation of Noise Field for Large Wave Number

Since we are expecting a spectrum rich in high harmonics, an approximate solution may be taken for the high frequency components as $h \rightarrow \infty$. Following again Hawkins and Lowson (Ref. 6), we use the stationary phase method.

The phase function under consideration is

$$f = \omega\left(\tau + \frac{\hat{r}}{a}\right) = \theta + \frac{\omega\hat{r}}{a}, \quad (27)$$

where \hat{r} is a function of (R, θ) , and

$$\hat{r} \approx \frac{r_0}{(1 - M^2)} \left\{ K_D - \frac{(1 - M^2) \sin \Omega}{(1 - M^2 \sin^2 \Omega)^{1/2}} \frac{R}{r_0} \cos \theta \right\}.$$

The stationary point (actually, a line) is:

$$\theta = \frac{3\pi}{2} ; \quad \frac{\omega R}{a} = \frac{(1 - M^2 \sin^2 \Omega)^{\frac{1}{2}}}{\sin \Omega} . \quad (28)$$

Since $\frac{\omega R}{a} = m$, one can see from equation (28) that the main contribution to the integral comes from a constant radius line where a ray is pointing directly toward the observer, as shown in Figure 7.

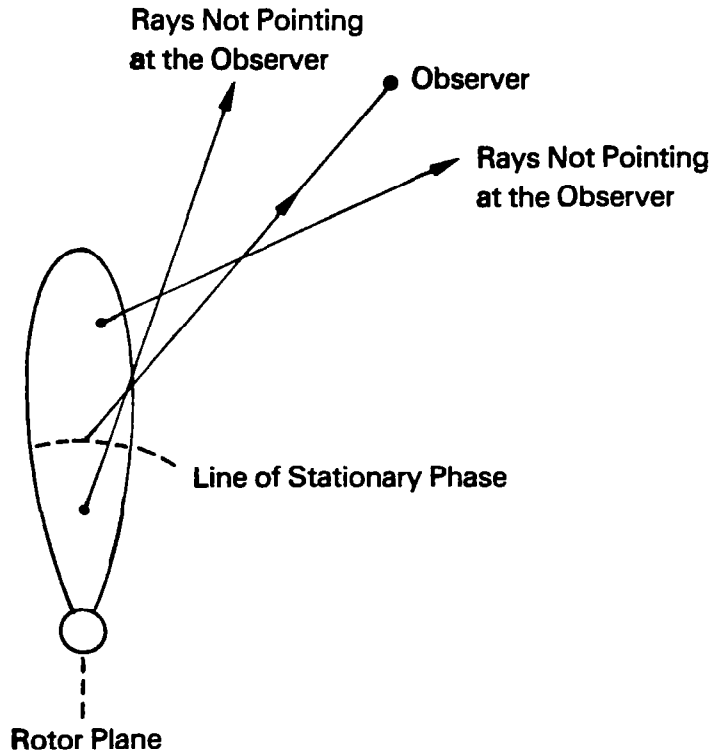


Figure 7. Radius of Stationary Phase and Ray.

For the thickness component, we obtain

$$(C_n)_h = \frac{i}{2\pi} \frac{(1 - M^2 \sin^2 \Omega)^{\frac{1}{2}} (1 - M^2)}{\sin \Omega K_D r_o} \exp \left\{ \frac{i3n\pi}{2} + \frac{i n \omega r_o K_D}{a(1 - M^2)} \right\} \\ \int \left[\rho_o a^2 (\vec{m} + \vec{M}) \cdot \nabla h \frac{R}{\cos \theta} \right]_{R=R_o} \exp(-in\phi) d\phi$$

with

$$R_o = \frac{a}{\omega} \frac{(1 - M^2 \sin^2 \Omega)^{\frac{1}{2}}}{\sin \Omega} \quad (29)$$

For the force components, we have

$$\begin{aligned}
(C_n)_{f_j} &= -\frac{1}{4\pi^2} \iint R \, dR \, d\phi \int d\phi \, f_j \frac{1}{r} \frac{\partial \hat{\psi}}{\partial x_j} \left(\frac{i\omega n}{a} \right) \exp \left(\theta + \frac{\hat{r}}{a} \right) \\
&= -\frac{i}{2\pi} \frac{(1 - M^2 \sin^2 \Omega)^{\frac{1}{2}}}{\sin \Omega} \exp \left\{ \frac{i3n\pi}{2} + \frac{i\omega r_o K_D}{a(a - M^2)} \right\} \\
&\quad \cdot \int \frac{1}{K_D r_o} \left\{ T \left[-\frac{\cos \Omega}{(1 - M^2 \sin^2 \Omega)^{\frac{1}{2}}} + M \right] \right. \\
&\quad \left. + \frac{D \sin \Omega (1 - M^2)}{(1 - M^2 \sin^2 \Omega)^{\frac{1}{2}}} \frac{R}{\cos \theta} \right\}_{R=R_o} e^{-in\phi} \, d\phi \quad . \quad (30)
\end{aligned}$$

Combining equations (29) and (30) results in the following:

$$\begin{aligned}
C_n &= \frac{i}{2\pi} \frac{(1 - M^2 \sin^2 \Omega)^{\frac{1}{2}} (1 - M^2)}{\sin \Omega K_D r_o} \exp \left\{ -\frac{in\pi}{2} + \frac{i\omega r_o K_D}{a(1 - M^2)} \right\} \\
&\int \left\{ \left[\rho_o a^2 (\vec{m} + \vec{M}) \cdot \nabla h + \frac{T}{(1 - M^2)} \left(\frac{\cos \Omega}{(1 - M^2 \sin^2 \Omega)^{\frac{1}{2}}} - M \right) \right. \right. \\
&\quad \left. \left. - \frac{D \sin \Omega}{(1 - M^2 \sin^2 \Omega)^{\frac{1}{2}}} \right] \frac{R}{\cos \theta} \right\}_{R=R_o} e^{-in\phi} \, d\phi \quad (31)
\end{aligned}$$

The asymptotic evaluation of the Fourier integral reduces the surface integral to a line integral on the chord, from where the main contribution comes. This reduces the computing time needed for the high frequency components of the spectrum.

OPTIMIZATION PROCEDURE FOR NOISE REDUCTION

Numerical optimization techniques have attained a high degree of refinement. However, very little is known to aid the selection of a particular optimization scheme for a given problem. In this study, we have evaluated several procedures to minimize the propeller-radiated noise which in principle could be implemented with any numerical optimization algorithm. The evaluation, however, was guided by our experience of utilizing the method of feasible directions and the conjugate gradient technique, as developed by Vanderplaats (Ref. 11) for constrained minimization problems. In this algorithm, the numerical search procedure is performed in the gradient directions to minimize the objective function while satisfying a set of constraints. For the advanced propeller problem we wish to minimize the noise level at a given point,

$$p(\vec{x}, t) = \sum_{n=-\infty}^{\infty} e^{-in\omega t} C_n(\omega, \vec{x}) \quad , \quad (32)$$

by varying some design parameters under some constraints. We assume that $p(\vec{x}, t)$ can be minimized by minimizing the Fourier components $C_n(\omega)$, and we will focus the discussion on minimization of $C_n(\omega)$ for a single harmonic frequency n . We have identified several procedures applicable for advanced transonic propellers as follows: a general noise minimization procedure involving all design parameters; an approximate noise minimization with propeller sweepback; and noise minimization for high frequency noise. In these procedures we assume that the observer is moving with the source (i.e., the observer is in the aircraft cabin) at a fixed lateral distance shortly aft of the propeller. Such a location is expected to have the highest radiated noise level, as illustrated in Figure 6.

General Noise Minimization Procedure

The noise function is given in terms of its Fourier components $C_n(\omega)$ and expressed in equation (20) which is repeated here for convenience:

$$\begin{aligned}
C_n = & \frac{i n \omega}{2 \pi a K_D r_o} \exp \left(\frac{i n \omega r_o K_D}{a(1-M^2)} - \frac{i n \pi}{2} \right) \cdot \iiint \underbrace{\left(\frac{a^2}{r_o} (\vec{m} + \vec{M}) \cdot \nabla h (1 - M^2) \right)}_{\text{Thickness}} \\
& + \underbrace{T \frac{\cos \Omega}{(1 - M^2 \sin^2 \Omega)^{\frac{1}{2}}} - M}_{\text{Thrust}} \left[\underbrace{- \frac{D(1 - M^2)}{m}}_{\text{Drag}} \right] \left. \vphantom{\frac{a^2}{r_o}} \right\} J_n(nY) \exp(-in\phi) (\cos \Theta)^{-1} R \, dR \, d\phi .
\end{aligned} \tag{20}$$

As identified, the first term in the surface integral of the equation includes the thickness distribution h , which is a function of its radial and angular location R and ϕ (see Figure 3). Likewise, the next two terms are the thrust and drag contributions. The incremental thrust and drag are also functions of each radial and angular location; i.e.,

$$h = h(R, \phi) , \tag{33a}$$

$$T = T(R, \phi) , \tag{33b}$$

$$D = D(R, \phi) , \tag{33c}$$

and finally the twist or pitch angle Θ is a function of the propeller radial station R :

$$\Theta = \Theta(R) . \tag{34}$$

If we describe the propeller with N radial and M angular stations, the optimization problem can then be stated as follows:

minimize $C_n(\omega)$ by varying the $N(3M + 1)$

design variables $h(R, \phi)$, $T(R, \phi)$, $D(R, \phi)$, and

$\Theta(R)$ subject to the following $N(M + 2) + 2$ constraints:

$$h(R_o, \lambda) \geq h_c(R_o, \lambda) \quad (\text{where } \lambda \text{ is the blade sweep}) \quad , \quad (35a)$$

$$\int T(R_o, \phi) \, d\phi \leq \int T_c(R_o, \phi) \, d\phi \quad , \quad (35b)$$

$$\iint T(R, \phi) \, R \, dR \, d\phi \geq T_o \quad , \quad (35c)$$

$$\text{and} \quad \iint R^2 D(R, \phi) \, dR \, d\phi \leq Q_o \quad . \quad (35d)$$

The first two N constraints express the structural requirement of minimum thickness and, having the loading below either a structural or aerodynamic maximum value at each radial location, the final two integral constraints express the integrated thrust and torque values to achieve the desired propeller performance.

The practicality of solving this problem will largely depend on the time required to compute the flow field around the propeller and to compute the gradient of the flow variables with respect to the $N(3M + 1)$ design variables. The simpler problem obviously is to consider only the variation of the propeller planform to noise as expressed by the thickness distribution.

Approximate Noise Minimization Procedure

In this approach we consider only the contribution of the thickness to the noise (i.e., only the first term in equation (20)). A first order approximation of the planform change by sweeping the propeller backward could be treated by computing the noise without regard to the coupled changes in the thrust and drag. This simplification essentially eliminates the flow field computation of thrust and drag and may provide a more feasible optimization procedure. In this procedure, the objective function to be minimized includes only the first term in the integral and only MN design variables are considered: $h(R_o, \phi)$ and $\Theta(R)$. The constraints are also reduced to N constraints on minimum thickness distribution at each radial location.

Another approach for an approximate optimization scheme may be considered by using the asymptotic solution to the high-frequency noise, as illustrated by equation (26).

Noise Minimization for High-Frequency Noise

In the asymptotic solution for the high-frequency noise (see equation (31)) most of the acoustic signature is assumed to be from a ray directed at the observer. The surface integral is then reduced to a line integral at the location for which the ray is directed towards the observer. Either the general noise minimization scheme or the approximate solution may

be applied with the asymptotic noise solution with considerable simplification. It should be recognized, however, that the solution would be a local solution relative to one observer, and numerous locations should be considered to redesign the overall propeller for optimum noise.

CONCLUSIONS

The prediction scheme outlined in this report is an extension of Hawkings and Lowson's (Ref. 6) work and is intended to facilitate the basic tool for the noise optimization in the design of advanced propellers.

The method gives some explicit directivity distribution. It gives good physical insight into the noise generation, particularly in defining the existence of the cone of silence, the Doppler amplification factor K_D and the critical radius for high-frequency components. In terms of numerical computation, the procedure is straightforward and fast, a factor of considerable importance for numerical optimization.

The method, however, is limited in some aspects. Except for the work by Hawkings and Lowson (Ref. 6), all the existing prediction methods, including this work, are based on linear theory. The nonlinear distortion of the wave form as it propagates from the emitter is not included. As pointed out by Hawkings and Lowson, the nonlinear effect is important in determining the spectrum, while linear theory may be sufficient in predicting the overall pressure level. The simplicity of the technique, however, is quite attractive for design purposes. A second limitation is due to the employment of the far field approximation. The observer at the cabin wall is roughly at 2.6 times the radius of the propeller. At such a close proximity the higher order term in the far field expansion may contribute significantly to the noise. Inclusion of the higher order terms can be carried out in the future. In many cases, the first term of an asymptotic expansion gives fairly good results for moderate parameter values. For the optimization scheme, the important feature is the ability to predict correctly the sensitivity of the function to the various design parameters. It is recommended that the initial optimization scheme be applied to the simplest noise prediction scheme.

A presentation of this work has been included in the Appendix.

Flow Research Company
A Division of Flow Industries, Inc.
Kent, Washington 98031
December 1, 1978

REFERENCES

1. Mikkelson, D. C.; Blaha, B. J.; Mitchell, G. A.; and Wikete, J. E.: Design and Performance of Energy Efficient Propellers for Mach 0.8 Cruise. NASA Technical Memorandum TM X-73612, 1977.
2. Baum, J. A.; Dumais, P. J.; Mayo, M. G.; Metzger, F. B.; Shenkman, A. M.; and Walker, G. G.: Prop-Fan Data Support Study, Technical Report. NASA CR-152141, 1978.
3. NASA. Energy Consumption Characteristics of Transports Using Prop-Fan Concept. NASA CR-137937, 1976.
4. Goldstein, M. E.: Aeroacoustics. National Technical Information Services NTIS N74-35118, 1974, pp. 230-244.
5. Ffowcs Williams, J. E.; and Hawkings, D. L.: Sound Generation by Turbulence and Surface in Arbitrary Motion. London: Proceedings of the Royal Society, Series A., vol. 264, 1969, pp. 321-342.
6. Hawkings, D. L.; and Lawson, M. V.: Theory of Open Supersonic Rotor Noise. Journal of Sound and Vibration, vol. 36, no. 1, 1974, pp. 1-20.
7. Farassat, F.; and Brown, T. J.: A New Capability for Predicting Helicopter Rotor and Propeller Noise Including the Effect of Forward Motion. NASA Technical Memorandum TM X-74037, 1977.
8. Whitham, G. B.: Linear and Non-Linear Waves. John Wiley & Sons, Inc., 1974.
9. Lawson, M. V.: The Sonic Field for Singularities in Motion. London: Proceedings of the Royal Society, Series A, vol. 286, 1965, pp. 559-572.
10. Lawson, M. V.; and Jupe, R. J.: Wave Forms for a Supersonic Rotor. Journal of Sound and Vibration, vol. 37, no. 4, 1974, pp. 475-489.
11. Vanderplaats, G. N.: CONMIN - A Fortran Program for Constrained Function Minimization User's Manual, NASA Technical Memorandum TM X-62282, 1973.

THE APPENDIX

**FLOW RESEARCH PRESENTATION NO. 104
PROCEDURE FOR NOISE PREDICTION AND
OPTIMIZATION OF ADVANCED
TECHNOLOGY PROPELLERS**

**Wen-Huei Jou
and
Sam Bernstein**

OBJECTIVES OF CONTRACT

- **Review Existing Theories of Propeller Noise**
- **Formulate a Prediction Scheme**
- **Formulate an Optimization Scheme for Noise Reduction**

OUTLINE OF PRESENTATION

- **Introduction: Past Analyses of Propeller Noise**
- **Extension of Hawkings and Lawson's Work to Include Forward Flight**
- **Optimization Procedure for Noise Reduction**
- **Conclusions**

CLASSIFICATION OF PROPELLER NOISE

- Multiple Pure Tone
- Wide Band Noise
- Blade Passing Tone

Gutin's Theory:

- Rotating dipole at center of force
- Theory breaks down for supersonic speed

$$\lambda/R = (a/\omega)/R = a/(\omega R) > 1$$

GENERAL THEORY OF FLOWCS WILLIAMS AND HAWKINGS

Sources	{	Volume Displacement	Monopole
		Surface Forces	Distributed Dipoles
		Stress Field	Distributed Quadrupoles

GENERAL SOLUTION (FFOWCS WILLIAMS AND HAWKINGS)

$$4\pi(p - p_0) = \partial^n / \partial x_i \partial x_j \dots \int Q_{ij\dots}(\vec{y}, \tau) [d(\tau - \tau_0)/r] d\vec{y} d\tau$$

$$r = |\vec{x} - \vec{y}|$$

$$\tau_0 = t - r/a$$

- General Space-Time Integral
- Dirac Delta Function Projects the Integral to Three-Dimensional Subspace
- Subspace Can Be Chosen at Will

GENERAL SOLUTION (CONT.)

- **Choose Physical Space as Subspace - Retarded Potential**
- **Choose a Sphere Centered at Observer and Collapsing at Sonic Speed (Sphere of Coincidental Arrival)**
 - Σ **Surface Solution or Collapsing Sphere Solution**

HAWKINGS AND LOWSON

- **Method**
 - **Retarded potential**
 - **Blade fixed coordinates for source space**
 - **Fourier analysis**
 - **Far field approximation**
- **Results**
 - **Qualitative directivity**
 - **Nonlinear distortion of time-wave form**
 - **For design purposes, linear theory is sufficient as a prediction tool**

FARASSAT

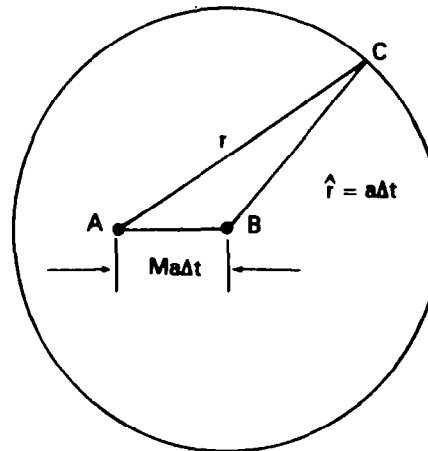
- **Method**
 - Collapsing sphere
 - Time domain
 - No far field approximation
- **Results**
 - Complete numerical computation for every field point
 - No qualitative directivity

PROPELLER NOISE WITH FORWARD FLIGHT

- Uniformly Convecting Velocity

$$\left[\frac{1}{a^2} \left(\frac{D^2}{Dt^2} - \nabla^2 \right) \right] p = \partial^n / \partial x_i \partial x_j \dots Q_{ij} \dots$$

- Wave Front is a Convected Sphere



$$\hat{r}/r = (K^2 + \beta^2)^{1/2} - K$$

$$K = (\vec{M} \cdot \vec{e}_r) \beta^2$$

$$\beta = (1 - M^2)^{-1/2}$$

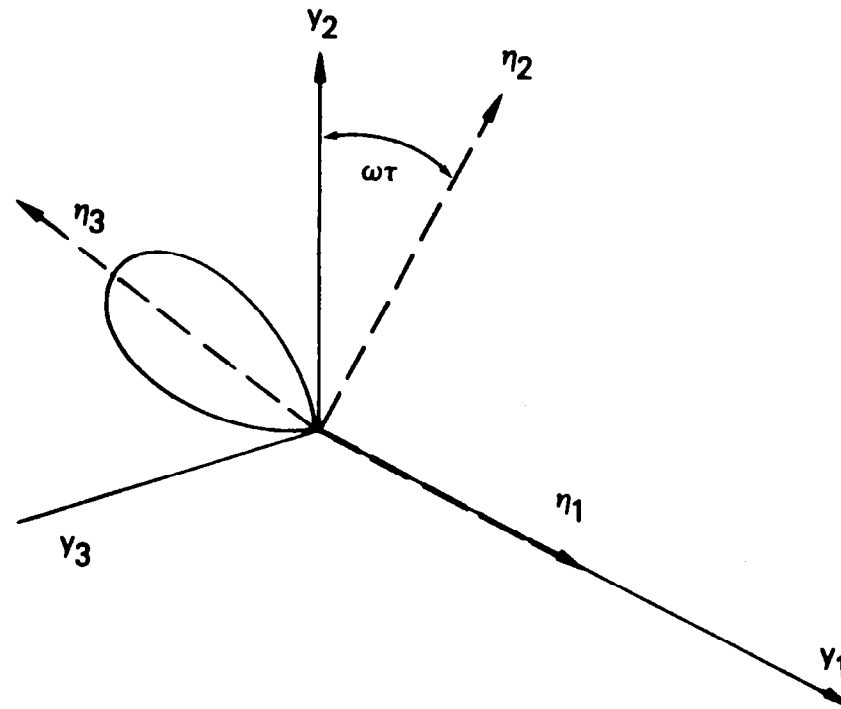
GENERAL SOLUTION TO CONVECTED WAVE EQUATION

$$4\pi(p - p_0) = \partial^n / \partial x_i \partial x_j \dots \int Q_{ij\dots}(\vec{y}, \tau) [\delta(\tau - \tau_0) / \hat{r}] d\vec{y} d\tau$$

$$\tau_0 = t - \hat{r}/a$$

TRANSFORMATION OF SOURCE SPACE TO BLADE FIXED COORDINATES

$$J = \det(\partial y_i / \partial \eta_j) = (1 + U_i \partial \tau / \partial y_i)^{-1}$$



RETARDED POTENTIAL SOLUTION ON BLADE FIXED COORDINATE

$$4\pi (p - p_0) = - \partial / \partial x_j \int [f_j / \hat{r}] J] dS$$

$$- \partial / \partial t \int [e_0 a(\vec{m} + \vec{M}) \cdot \nabla h / \hat{r} \cdot J] dS$$

S: Blade Surface

FOURIER COMPONENTS

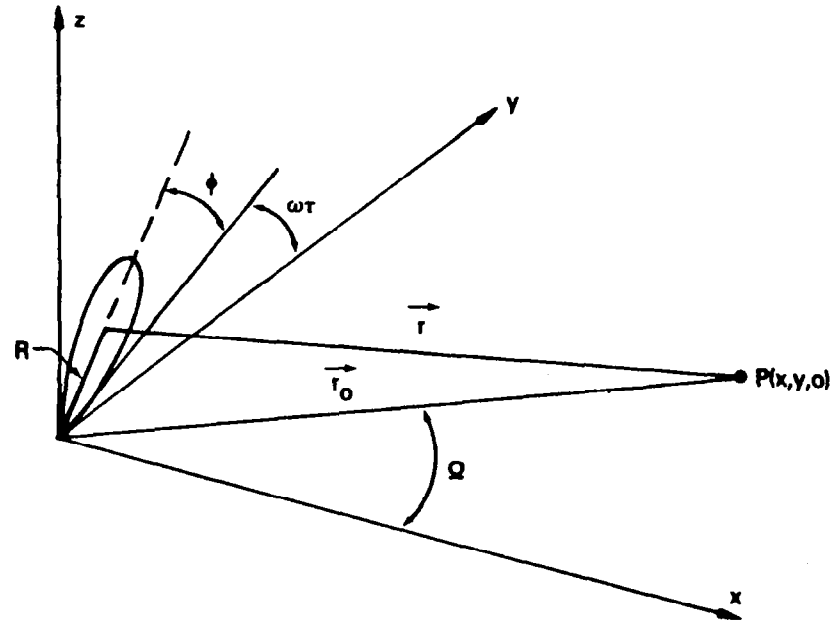
$$\begin{aligned} C_n &= \int (p - p_0) e^{in\omega t} dt \\ &= \int (p - p_0) e^{in\omega(\tau + r/a)} (dt/d\tau) d\tau \end{aligned}$$

$$\tau + \Delta t [\vec{y}(\tau)] = t$$

$$dt = J^{-1} d\tau$$

FOURIER COMPONENTS (CONT.)

- Polar Coordinate



- Far Field Approximation

$$(R/r) \ll 1 ; (a/n\omega r) \ll 1$$

- $C_n = (C_n)_h + (C_n)_f$

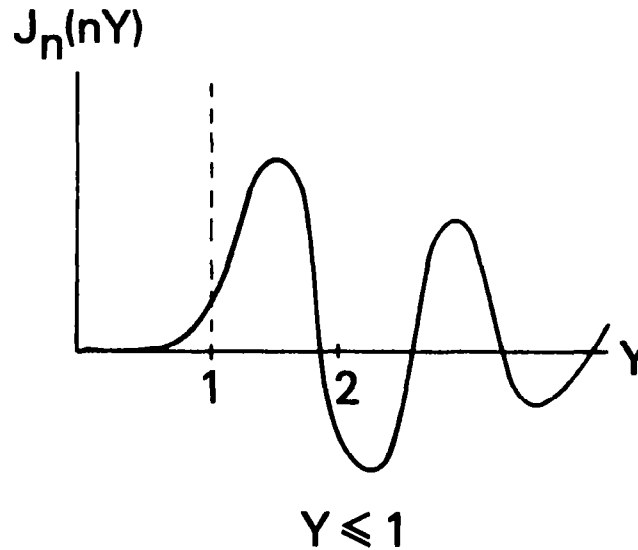
FOURIER COMPONENTS (CONT.)

$$(C_n)_h = A/(K_D r_0) \iint (\vec{m} + \vec{M}) \cdot \nabla h J_n(nY) \exp(-in\phi) [R/\cos\Theta] d\phi dR$$

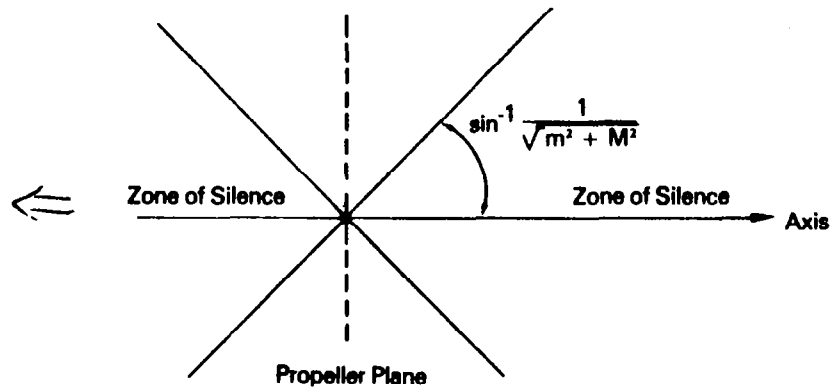
$$Y = m \sin \Omega / (1 - M^2 \sin^2 \Omega)^{1/2}$$

QUALITATIVE DIRECTIVITY

I. Zone of Relative Silence

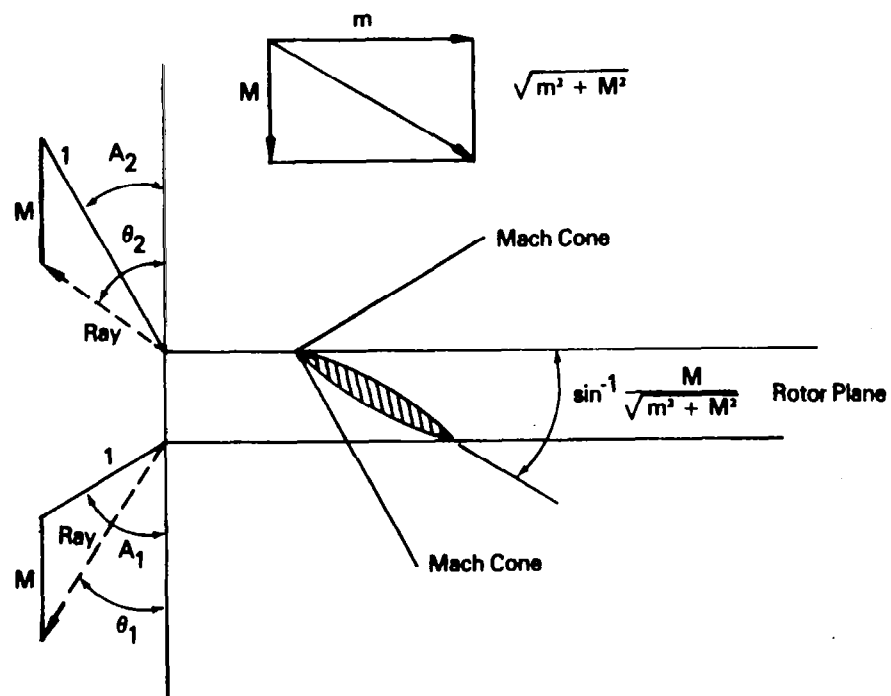


$$\Omega \leq \sin^{-1} \left[1 / (m^2 + M^2)^{1/2} \right] = \sin^{-1} \left[1 / M_{\text{tip}} \right]$$



QUALITATIVE DIRECTIVITY (CONT.)

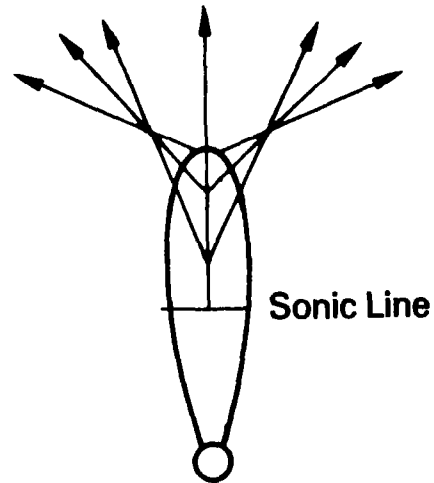
- Wave Kinematics (Hayes)



$$\theta_1 = \theta_2 = \sin^{-1} \left[\frac{1}{(m^2 + M^2)^{1/2}} \right]$$

QUALITATIVE DIRECTIVITY (CONT.)

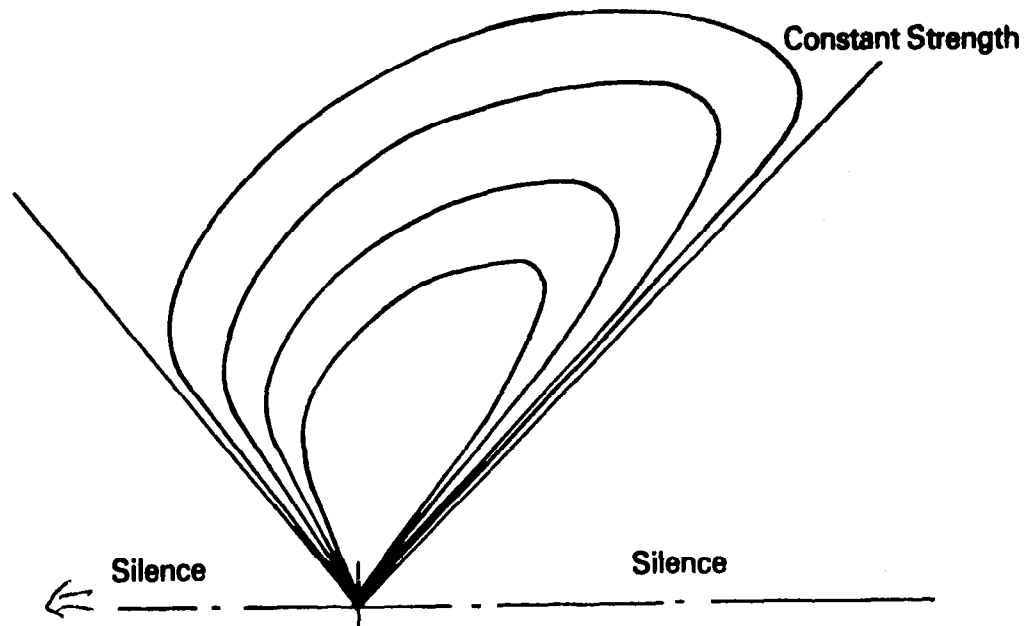
- Wave Kinematics (Cont.)



QUALITATIVE DIRECTIVITY (CONT.)

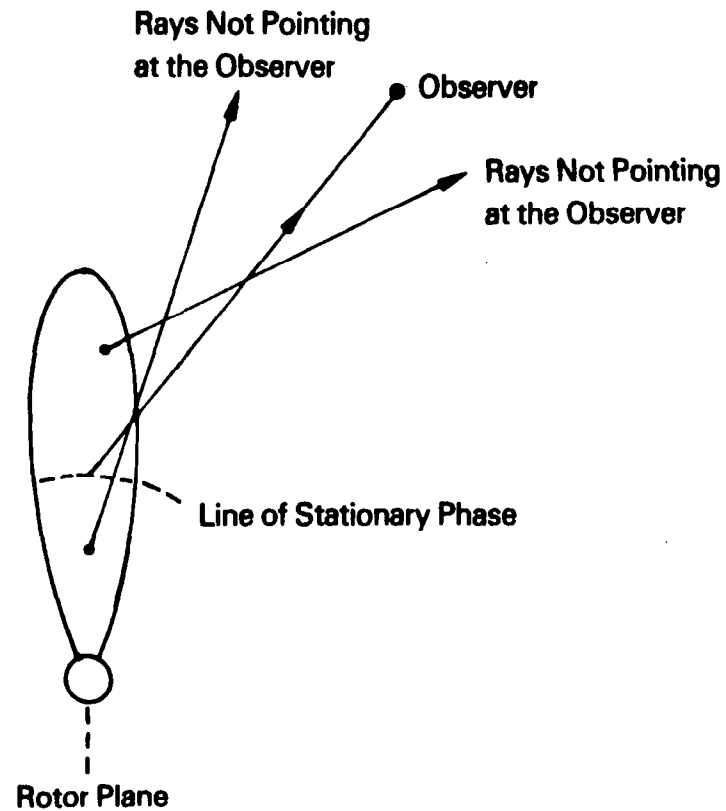
II. Doppler Amplification

$$1/K_D = \left\{ (1 - M^2 \sin^2 \Omega)^{1/2} - M \cos \Omega \right\}^{-1}$$



HIGH FREQUENCY APPROXIMATION

$$R_o = a/\omega \left[(1 - M^2 \sin^2 \Omega)^{1/2} / \sin \Omega \right]$$



SUMMARY OF NOISE COMPUTATION PROCEDURE

$$P(\vec{x}, t) = \sum_{n=-\infty}^{\infty} e^{in\omega t} C_n(\omega, \vec{x})$$

$$C_n(\omega) = K(\omega, K_D, M, n) \iint \left\{ \underbrace{\rho_0 a^2 (m + M) \cdot \nabla h (1 - M^2)}_{\text{Thickness}} \right. \\ \left. + \underbrace{T [\cos \Omega / (1 - M^2 \sin^2 \Omega)^{1/2} - M]}_{\text{Thrust}} - \underbrace{D (1 - M^2) / m}_{\text{Drag}} \right\}$$

$$\cdot J_n(nY) \exp(-in\phi) (R/\cos \Theta) dR d\phi$$

$$h = h(R, \phi)$$

$$T = T(R, \phi)$$

$$D = D(R, \phi)$$

$$\Theta = \Theta(R)$$

OPTIMIZATION PROCEDURE FOR NOISE REDUCTION

**Minimize $C_n(\omega)$ by Varying $h(R,\phi)$, $T(R,\phi)$, $D(R,\phi)$, and $\Theta(R)$
Subject to the Following Constraints:**

- **Thickness distribution is longer than minimum value at each radial location (structural)**
- **Integrated thrust at each radial location is lower than a given maximum allowable load (structural/aerodynamic)**
- **Integrated thrust sufficient for aircraft propulsion**
- **Integrated torque compatible with available engine power**

